

Haverford College

Haverford Scholarship

Faculty Publications

Astronomy

1991

Limits on Gaussian fluctuations in the cosmic microwave background at 19.2 GHz

Stephen P. Boughn

Haverford College, sboughn@haverford.edu

E. S. Cheng

D. A. Cottingham

D. J. Fixsen

Follow this and additional works at: https://scholarship.haverford.edu/astronomy_facpubs

Repository Citation

"Limits on Gaussian Fluctuations in the Cosmic Microwave Background at 19.2 GHz (with E. Cheng, D. Cottingham, and D. Fixsen), *After the First Three Minutes*, S. Holt, C. Bennett, and V. Timble (eds.) (American Institute of Physics, New York, 1991), pp. 107-112.

This Book is brought to you for free and open access by the Astronomy at Haverford Scholarship. It has been accepted for inclusion in Faculty Publications by an authorized administrator of Haverford Scholarship. For more information, please contact nmedeiro@haverford.edu.

LIMITS ON GAUSSIAN FLUCTUATIONS IN THE COSMIC MICROWAVE BACKGROUND AT 19.2 GHz

S. P. BOUGHN

Strawbridge Observatory, Haverford College, Haverford, PA 19041

E. S. CHENG

NASA/Goddard Space Flight Center, Building 21-G54, Code 685.0, Greenbelt, MD 20771

D. A. COTTINGHAM¹

Center for Particle Astrophysics, University of California, Berkeley

AND

D. J. FIXSEN

NASA/Goddard Space Flight Center, Code 685.3, Greenbelt, MD 20771

Received 1990 October 23; accepted 1992 March 12

ABSTRACT

The northern hemisphere data from the 19.2 GHz full sky survey are analyzed to place limits on the magnitude of Gaussian fluctuations in the cosmic microwave background implied by a variety of correlation functions. Included among the models tested are the monochromatic and Gaussian-shaped families, and those with power-law spectra for $-2 \leq n \leq 1$. We place an upper bound on the quadrupole anisotropy of $\Delta T/T < 3.2 \times 10^{-5}$ rms, and an upper bound on scale-invariant ($n = 1$) fluctuations of $a_2 < 4.5 \times 10^{-5}$ (95% confidence level). There is significant contamination of these data from Galactic emission, and improvement of our modeling of the Galaxy could yield a significant reduction of these upper bounds.

Subject heading: cosmic microwave background

1. INTRODUCTION

Theories which attempt to trace the evolution of the present extremely inhomogeneous large-scale distribution of luminous matter in the universe have, as a general feature, implications about the size and form of anisotropies in the cosmic microwave background (CMB). Many of these theories of structure formation suggest that the fluctuations in the CMB would take the form of a two-dimensional random Gaussian field; other theories, notably those involving stringlike defects in the vacuum, lead to non-Gaussian statistics. To settle observationally the question of which of these theories is correct, and in particular whether the fluctuations are described by Gaussian statistics or not, will require an accurate measurement of the two- and three-point correlation functions of the anisotropy. There are at present no verified detections of any anisotropy (other than Sunyaev-Zel'dovich, a relatively local effect), much less a measured correlation function, so observational results thus far take the form of upper limits. However, the observed high level of isotropy of the CMB is already an important constraint on these theories.

In this *Letter* we present an analysis of the limits that can be set on fluctuations at angular scales greater than 1° by the northern hemisphere portion of the 19.2 GHz survey (Cottingham 1987; Boughn et al. 1990, 1992). This survey was carried out at an angular resolution of 3° FWHM and a typical sensitivity of 1.5 mK per resolution element. The northern hemisphere portion covers declinations $-15^\circ < \delta < +75^\circ$.

We consider only fluctuations which obey Gaussian statistics. A Gaussian field is completely specified by its two-point correlation function. As we discuss further, the upper limit that

a given experiment can place on the rms fluctuation depends on the assumed correlation function. To preserve this distinction, all of our results are stated as pertaining to a particular correlation function, and not just to an angular scale. Many

conventions have been used for quoting the magnitude of fluctuations. We quote the size of fluctuations as $\Delta T/T$ rms (with one noted exception). This convention is shared by others, e.g., Timbie & Wilkinson (1990) and Readhead et al. (1989). In § 2 we discuss the method of statistical analysis employed, and the manner in which the data set is prepared. The various correlation functions tested and the upper limits obtained are presented in § 3.

2. ANALYSIS

The method we use to place an upper bound on the magnitude of fluctuations present in the data is the familiar one of selecting a statistic, and seeing where the measured value of this statistic falls on the distribution predicted by a particular model. The rms of fluctuations in the model is adjusted so that the probability that we would have measured a larger value of the statistic is equal to the confidence level (say, 0.95); we then know that if the rms were larger than this value, our observation would be quite unlikely (probability < 0.05) so this value of rms is a reasonable upper bound. A statistic is simply a function of the observations, so in order to determine its distribution we first need to know how the model predicts the observations are distributed.

Let $T(\theta, \varphi)$ describe the temperature fluctuations in the sky predicted by a given model. A Gaussian model is completely specified by its correlation function $C(\theta)$. We find it convenient to separate the shape of $C(\theta)$ from its magnitude; therefore we set $C(0) = 1$, so that the actual correlation function is $\eta^2 C(\theta)$ where η is the total rms fluctuation predicted by the

¹ Present address: NASA/Goddard Space Flight Center, Code 685.3, Greenbelt, MD 20771.

model [i.e., with this convention the mean square fluctuation $\langle (1/4\pi) \int d\Omega T^2(\theta, \varphi) \rangle$ is identically η^2]. Then

$$\langle T(\theta_1, \varphi_1) T(\theta_2, \varphi_2) \rangle = \eta^2 C(\theta_{12}), \quad (1)$$

where θ_{12} is the angle between the directions (θ_1, φ_1) and (θ_2, φ_2) . If we expand $C(\theta)$ and $T(\theta, \varphi)$ in spherical harmonics using the convention

$$C_l = 2\pi \int d(\cos \theta) C(\theta) P_l(\cos \theta) \quad (2)$$

$$T_{lm} = \int d\Omega Y_{lm}(\theta, \varphi) T(\theta, \varphi), \quad (3)$$

then from the above it follows that

$$\langle T_{lm} T_{l'm'}^* \rangle = \delta_{ll'} \delta_{mm'} \eta^2 C_l. \quad (4)$$

The antenna gain pattern for our instrument is approximately azimuthally symmetric. Let the relative antenna gain at angle θ from the axis be $H(\theta)$. For each observation we direct the antenna toward a point in the sky (θ_i, φ_i) and record the observed temperature s_i , given by

$$s_i = \int d\Omega_1 T(\theta_1, \varphi_1) H(\theta_{i1}). \quad (5)$$

If $H(\theta)$ is expanded in Legendre polynomials as we did $C(\theta)$ above, we obtain

$$s_i = \sum_{lm} H_l T_{lm} Y_{lm}(\theta_i, \varphi_i). \quad (6)$$

The correlation matrix of the s_i is then

$$\langle s_i s_j \rangle = \eta^2 \sum_l H_l^2 C_l \frac{2l+1}{4\pi} P_l(\cos \theta_{ij}) \equiv \eta^2 C'(\theta_{ij}), \quad (7)$$

where $C'(\theta)$ is then the correlation function smoothed by the antenna gain pattern. [Note that our convention $C(0) = 1$ does not imply $C'(0) = 1$.]

The instrument adds noise to the sky observations s_i ; thus, the actual observed value is $t_i = s_i + n_i$, where n_i is the instrumental noise. The noise is approximately uncorrelated, so $\langle n_i n_j \rangle = \delta_{ij} \sigma_i^2$, and is also not correlated with the sky fluctuations, so

$$\langle t_i t_j \rangle = \eta^2 C'(\theta_{ij}) + \delta_{ij} \sigma_i^2 \equiv M_{ij} \quad (8)$$

is the correlation matrix of the observations. The joint probability density (or likelihood function) of the observed values is then

$$L(t_1, \dots, t_n; \eta) = [(2\pi)^N \det M]^{-1/2} \exp\left(-\frac{1}{2} \sum_{ij} t_i t_j M_{ij}^{-1}\right). \quad (9)$$

Having derived the probability distribution of the observations, we move now to the selection of a statistic. The statistic that we use to compare the observations t_i to a model described by the correlation function $C(\theta)$ is

$$S = \sum_{ij} \frac{t_i t_j}{\sigma_i^2 \sigma_j^2} C'(\theta_{ij}). \quad (10)$$

This statistic was motivated as an approximation to the likelihood ratio (Martin 1971), the computation of which is intractable on our data. (Specifically, if the likelihood ratio is λ , then S is the first nonvanishing term in the expansion of $2/\eta^2 \ln \lambda$ in

orders of η , minus an irrelevant constant.) However, we make no assumption that S is approximately the likelihood ratio. We determine the distribution of S , given that the t_k are distributed according to (9), by Monte Carlo analysis. Once we know this distribution as a function of η and our measured value of S , we can then find the value of η which is excluded at a given confidence level.

It is interesting to compare these upper bounds with the upper bounds one would, in some sense, expect from the experiment. One can derive the probability distribution of S under the assumption that there are no fluctuations in sky temperature by the same Monte Carlo method; the median value of this distribution is a good estimate of the expected value of S in the absence of fluctuations. An upper bound on the rms derived using this value for S as the ‘‘measured value’’ is then a reasonable definition of the ‘‘expected upper bound.’’ We refer to this upper bound as the ‘‘upper bound sensitivity’’ of the experiment. A statistician would refer to this definition as the level of fluctuations for which the power of a given confidence level test is 50%. A large discrepancy between the upper bound sensitivity and the actual upper bounds obtained indicates that some correlation is present in the data; if the correlation is due to contamination by systematic effects or foreground sources, the upper bound sensitivity indicates the best that can be achieved by learning how to correct for the contamination, if no actual CMB fluctuation is encountered. We present both the upper bound and upper bound sensitivity for each model tested.

The upper limits quoted in this *Letter* are based on 200 Monte Carlo samples. From examining the scatter between different runs, we conclude that this is sufficient to locate the correct 95% confidence level to within $\pm 5\%$. Those results which are presented only in graphical form are based on 100 samples, which should be correct to $\pm 10\%$. In addition, the calibration of the 19.2 GHz survey is accurate to 3%, and the instrumental noise is measured to 5%, giving a total systematic error of $\pm 8\%$.

The data for the northern hemisphere are prepared by subtracting an a priori model of Galactic emission. This model was constructed by scaling the 408 MHz survey (Haslam et al. 1982) with a spectral index of -2.75 . To this was added a compilation of bremsstrahlung sources which had been normalized by fitting to the 25.4 GHz survey (Fixsen 1982; Fixsen, Cheng, & Wilkinson 1983) and then scaled to 19.2 GHz with a spectral index of -2.1 . In those portions of the sky where comparison is possible (i.e., in the Galactic plane), the model agrees with our observations to within a factor of 2. This poor agreement suggests that there may be significant Galactic emission off the plane which this model does not remove. We then fit and remove the constant and dipole components. The portion within 20° of the Galactic plane is removed, as well as the region near Orion.

3. RESULTS

In this section we present the results of comparing several correlation functions to the data. Since a least-squares best-fit dipole and offset is subtracted from the data, the correlation functions also have these components removed. Since our coverage of the sky is not uniform, it is not sufficient to simply eliminate the $l = 0$ and 1 components when constructing the Monte Carlo samples; for each sample we determine a least-squares best-fit dipole and offset and subtract it.

We first compare our data to two families of generic models. Generic correlation functions are conveniently parameterized by an angular scale; we adopt the convention that the angular scale θ_0 is the correlation length, defined by

$$\theta_0^{-2} = - \left[\frac{1}{C} \frac{d^2 C}{d\theta^2} \right]_{\theta=\theta_0}. \quad (11)$$

[Note that with this convention the angular scale θ_0 of correlation functions which exclude the $l = 0$ and 1 components cannot exceed the correlation angle of a quadrupole, which is $(1/3)^{1/2}$ radians or about 33° ; thus the plots in Fig. 1 end at this angle.] The first family of generic models, dubbed monochromatic, are defined as having only one nonzero component of the power spectrum C_l ; then $C(\theta) = P_l(\cos \theta)$, and thus $C'(\theta) = H_l^2 P_l(\cos \theta)$. The correlation length for the monochromatic models is $\theta_0 = [2/l(l+1)]^{1/2}$. The second generic family is called Gaussian-shaped because the power spectrum has the shape of a Gaussian function; this use of the term ‘‘Gaussian’’ should not be confused with its use in describing the statistics of the fluctuations. These models are defined by

$$C_l = N e^{-l^2/2l_0^2}, \quad l \geq 2, \quad (12)$$

where N is a constant chosen to normalize $C(0) = 1$. For large values of l_0 the correlation angle is roughly $\theta_0 \approx 1/l_0$.

The results of testing monochromatic and Gaussian-shaped models are shown in Figures 1a and 1b, respectively. These figures also show the upper bound sensitivity (as defined in § 2) of our experiment to fluctuations of these forms. Note in particular that the upper limit on the amplitude of a quadrupole ($l = 2$) anisotropy is $\Delta T/T < 2.8 \times 10^{-5}$ rms; the upper bound sensitivity to the quadrupole is $\Delta T/T < 3.2 \times 10^{-5}$ rms. In cases (such as this one) where the upper bound is less than the upper bound sensitivity, we prefer to quote the more conservative number. The fact that the limits we have set are in many other cases so far above the sensitivity of the experiment is a clear indication that the map is correlated. It is apparent that we have detected the presence of fluctuations in our data, but the magnitude of Galactic emission in these data and the poor fit of our Galactic model in those regions of the map where comparison is possible preclude positive identification of these fluctuations as CMB anisotropy. The possibility that the detected anisotropy is due to Galactic emission is supported by

TABLE 1
UPPER LIMITS ON a_2 FOR POWER-LAW
SPECTRUM MODELS

n	Upper Bound ($\Delta T/T \times 10^6$)	Sensitivity ($\Delta T/T \times 10^6$)
+1.....	45	19
0.....	53	27
-1.....	50	32
-2.....	42	38

the fact that both the upper and lower bounds on all models examined increase significantly when the width of the Galactic plane cut is decreased.

Many theoretical models have as their large angular scale limit a power law spectrum. For these models, the correlation function is given by (Bond & Efstathiou 1987)

$$C_l = (a_2)^2 \frac{\Gamma(l + [n - 1]/2)\Gamma([9 - n]/2)}{\Gamma(l + [5 - n]/2)\Gamma([3 + n]/2)} \quad n < 3, \quad l \geq 2, \quad (13)$$

and $C(\theta) \approx \theta^{1-n}$. The $n = 1$ case corresponds to scale-invariant fluctuations in two dimensions. For these models we deviate from our practice of quoting an upper limit on the total rms fluctuation, necessitated by the fact that for $n > 0$ these models have infinite rms. Instead, we quote an upper limit on the parameter a_2 . Our 95% confidence level upper limits and upper bound sensitivities are presented in Table 1.

It has been common practice to use the upper bound on the quadrupole as a limit on a_2 ; to make the conversion, one uses the fact that $a_2 = (4\pi/5)^{1/2} \times \text{rms}$ of the quadrupole alone. [For a quadrupole $C(\theta) = P_2(\cos \theta)$, and eq. (2) then implies $C_2 = 4\pi/5$; in our notation $a_2 = \eta(C_2)^{1/2} = (4\pi/5)^{1/2} \times \text{rms}$.] The limit on a_2 that would be derived in this way from our upper bound on the quadrupole is $a_2 < 5.1 \times 10^{-5}$. We note that this is not much different from any of the values listed in Table 1.

For most of the models we have presented, the upper bound sensitivity of the experiment is well below the upper bound that we are able to set, suggesting that if we are able to improve the removal of foreground emission, we may be able to significantly lower these upper bounds.

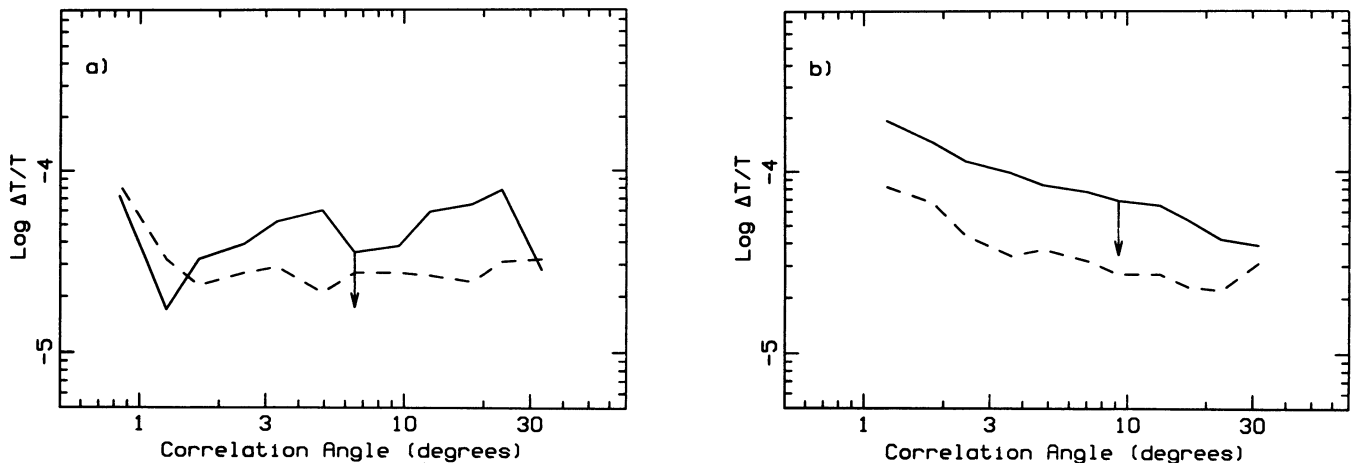


FIG. 1.—Upper bounds on $\Delta T/T$ rms (95% confidence level). (a) Monochromatic models, (b) Gaussian-shaped models. In both, the solid line is the 95% confidence level upper bound, and the dashed line is the upper bound sensitivity of this experiment, as defined in the text.

We would like to thank Steve Meyer, Lyman Page, Jeff Peterson, Peter Timbie, Juan Uson, and Nicola Vittorio for many helpful discussions. This work received a great deal of guidance and support from David Wilkinson. We also benefited from the discussions at the 1990 Winter Physics Conference at the Aspen Center for Physics. The observations on

which these results are based were taken at the National Scientific Balloon Facility in Palestine, Texas. Princeton University was the home of this project at its inception and through the gathering of the northern hemisphere data. This work was supported by NASA and in part by the NSF.

REFERENCES

- Bond, J. R., & Efstathiou, G. 1987, MNRAS, 226, 655
 Boughn, S. P., Cheng, E. S., Cottingham, D. A., & Fixsen, D. J. 1990, Rev. Sci. Instr., 61, 158
 ———. 1992, in preparation
 Cottingham, D. A. 1987, Ph.D. thesis, Princeton Univ.
 Fixsen, D. J. 1982, Ph.D. thesis, Princeton Univ.
 Fixsen, D. J., Cheng, E. S., & Wilkinson, D. T. 1983, Phys. Rev. Lett., 50, 620
 Haslam, C. G. T., Salter, C. J., Stoffel, H., & Wilson, W. E. 1982, A&AS, 47, 1
 Martin, B. R. 1971, Statistics for Physicists (London: Academic)
 Readhead, A. C. S., Lawrence, C. R., Myers, S. T., Sargent, W. L. W., Hardebeck, H. E., & Moffett, A. T. 1989, ApJ, 346, 566
 Timbie, P. T., & Wilkinson, D. T. 1990, ApJ, 353, 140